scientific reports

Check for updates

OPEN

gdf11 is required for pronephros/cloaca development through targeting TGF-β signaling

Xinning Tian[1,2], Wantao Yao[1,2], Jin Tan[1,2], Zhangle Hu[1]✉ & Jingwen Liu[1,2]✉

The kidney is a vital organ responsible for removing toxins, producing urine, and regulating homeostasis. Developmental defects in the kidney lead to various congenital abnormalities that impair renal function. Gdf11, a member of the transforming growth factor β family, is associated with numerous renal abnormalities. In the early developmental stage, the pronephric duct and hindgut open into the cloaca, and Gdf11 shows significant expression in the hindgut of mice. However, the molecular and cellular roles of *gdf11* in kidney and cloaca organogenesis remain unclear. Our study revealed that pronephros and cloaca formation were significantly disrupted upon *gdf11* deletion or knockdown in zebrafish. Additionally, we found that the TGF-β pathway acts downstream of Gdf11 in promoting pronephros and cloaca development. Treatment with a TGF-β small molecule activator partially rescued the pronephros and cloaca developmental defects observed in *gdf11*$^{-/-}$ mutants. In summary, our findings provide strong evidence of a critical link between pronephros/cloaca formation and TGF-β signaling mediated by Gdf11. Our study also provides new insight into diseases related to renal and cloaca development.

Keywords Gdf11, Zebrafish, TGF-β, Pronephros, Cloaca

The kidney is essential for waste removal and the regulation of fluid homeostasis in the body[1]. Kidney development is a complex process that involves multiple signaling pathways, including Wnt, Notch, MAPK/ERK, JAK/STAT, FGF, BMP, and TGF-β[2–7]. In lower vertebrates, the pronephros functions as the initial filtration unit. The zebrafish larval kidney, or pronephros, contains two nephrons consisting of glomerulus, the proximal convoluted tubule (PCT), the proximal straight tubule (PST), the distal early tubule (DE), and the distal late segment (DL)[8,9]. The cloaca serves as the shared opening for the urinary and gastrointestinal tracts to the external environment. The formation of the cloaca requires epithelial cell remodeling and apoptosis of epidermal cells to facilitate duct opening. If the this process goes wrong, pronephric duct cells cannot penetrate the ectodermal layer and thus cloaca fail to open[10,11].Previous research reports that Shh, BMP, and Wnt signaling pathways play roles in cloaca development in zebrafish[11–13]. Understanding the molecular mechanisms involved in pronephros and cloaca formation is vital for guiding future research.

Growth differentiation factor 11 (GDF11), a critical signaling protein of the TGF-β family, is essential for normal development, aging, and cancer[14]. Recent studies suggest that Gdf11 is also a key factor in the development of the metanephric kidney by inducing Gdnf expression, and Gdf11 deletion leads to kidney fibrosis in mice[15,16]. Additionally, Gdf11 is expressed in the hindgut and is implicated in anorectal malformations[17]. Despite these findings, the molecular mechanisms by which Gdf11 functions in development remain largely unexplored.

In our study, we aimed to assess the molecular impact of Gdf11 on pronephros and cloaca formation. We observed that *gdf11* knockout significantly compromised pronephros and cloaca function in zebrafish. Furthermore, deletion or suppression of *gdf11* expression resulted in a decrease in the expression of genes associated with the pronephros and an impairment of pronephric duct specification in zebrafish. Consistent with these findings, cloaca formation was notably affected in *gdf11* mutant and morphant embryos. Importantly, we found that the TGF-β signaling pathway was involved in pronephros and cloaca development downstream of *gdf11*. Based on these findings, we demonstrated that treatment with a TGF-β signaling activator could partially rescue defects in pronephros and cloaca formation of *gdf11* mutants. Our results suggest that Gdf11 supports pronephros and cloaca organogenesis through TGF-β signaling, providing new insights into related renal and cloaca diseases.

[1]Department of Cardiology, the Second Affiliated Hospital of Anhui Medical University, Hefei 230601, China. [2]School of Basic Medicine, Anhui Medical University, Hefei 230032, China. ✉email: lovecardiof@163.com; 1205099802@qq.com

Materials and methods

Animal models

The adult wild-type zebrafish of AB strain was purchased from China Zebrafish Resource Center (http://www.zfish.cn/). Adult wild-type zebrafish and embryos were raised under standard laboratory conditions. Embryos were maintained in Holtfreter's solution at 28.5 °C and staged according to morphological criteria. *gdf11* mutants, constructed and utilized in prior experiments, were included in this study[18].

Morpholinos and microinjection

Control and *gdf11* MO were synthesized by Gene Tools (Philomath, USA) and diluted to a concentration of 1 mM in nuclease-free water. The *gdf11* MO sequence was 5'-ATACCTTTTCATGTTGTTAAATATC-3'[19], while the 5 bp mismatch control MO sequence was 5'-ATAGCTTTTGATCTTCTTAAAAATC-3'. *gdf11* expression in zebrafish was knocked down by injecting *gdf11* MO at 4 ng/embryo.

Whole-Mount in situ hybridization

Whole-mount in situ hybridization was performed using the NBT-BCIP substrate according to previously established protocols[20]. Zebrafish embryos were harvested at indicated stages and fixed with 4% PFA (paraformaldehyde) overnight. These embryos could be stored at -20℃ after graded dehydration in methanol for long time. For WISH, zebrafish embryos were rehydrated in PBST buffer, and pre-hybridizated with HYB^- buffer at 65 ℃ for 15 min. After that, these embryos were hybridizated with HYB^+ buffer at 65 ℃ overnight. At the second day, zebrafish embryos were washed with 50% formamide/ 2xSSCT, 2xSSCT, 0.2x SSCT buffer sequentially. After inactivated goat serum blocking for 1 h, Digoxigenin-AP antibody (11093274910, Roche, 1:3000) was used to incubate with embryos overnight at 4 ℃. At the 3rd day, MABT buffer was employed to wash embryos for many times. After that, embryos were visualized with substrate BM-Purple (11442074001, Roche) and imaged with Nikon SMZ18 research-grade stereomicroscope. Digoxigenin-UTP – labeled RNA probes were transcribed from a linearized plasmid in vitro with RNA Polymerase T7/Sp6 system (10881775001/11487671001,Roche) and the primer sequences for probe amplification are listed in Table S1.

Renal filtration

Wild type or mutant embryos were anaesthetised with 2% tricaine (E10521, Sigma-Aldrich) at 56 hpf. After that, embryos were immobilised in 2.5% methyl cellulose, and were injected with 1 nl Tetramethylrhodamine-labeled dextran (70,000 MW; Invitrogen, Carlsbad, CA) into the pericardium, following previously described procedures[21]. Embryos were imaged Nikon A1R + confocal microscope immediately post-injection, at 61 hpf, and at 80 hpf. These images were processed with Nikon NIS-Elements ver. 5.20 software.

Cloaca excretion assay

Both wild-type and mutant embryos were injected with fluorescent rhodamine dextran (Molecular Probes) at 4 dpf and imaged with Nikon A1R + confocal microscope, consistent with previous report[11].

Cell Preparation

The HEK 293T cell line (Cell Bank, Shanghai, China) was cultured in DMEM supplemented with 10% fetal bovine serum at 37 °C in a humidified incubator with 5% CO_2. Primers used for plasmid construction are listed in Table S2. Transfections were performed using Lipo3000 (L3000008, Thermo Fisher) method for HEK293T cell.

Western blotting

For Western blotting, we first remove the medium in dish and wash with PBS buffer. After that, RIPA lysis buffer (R0010, Solarbio, Beijing, China) was added with protease inhibitor and placed in a mixer for 10 min. After mixing, the lysate was centrifuged at 4 °C 12,000 rpm for 5 min, then we collected the supernatant, add 6 × protein loading buffer. After that, these lysates were placed in heat bath at 100 °C for 5 min. Protein lysates were separated by SDS-PAGE. After SDS-PAGE, the membrane was transferred and blocked with skimmed milk for 1 h. After blocking, the membrane was incubated with primary antibody overnight. After the primary antibody incubation, the membrane was washed with MABT solution three times for 10 min each time. Next, the membrane was incubated with secondary antibody for one hour, and the membrane was washed with MABT solution three times for 10 min each time. The bands were imaged with ChemiDoc MP Imaging System. The primary antibodies were listed in Table S3.

For Western blot after FACS, zebrafish embryos were anesthetized, and then we used a needle to roughly cut the pronephros and cloacal area of the *Tg (cdh17-dsRed)* transgenic embryos on the ice under a fluorescence microscope. Approximately 300–400 embryos were processed at the same time. After FACS, RIPA buffer and dephosphorylase inhibitors were added to these cells following Western blot process. The primary antibody concentrations for p-Smad2 and p-Smad3 were adjusted to 1:80.

Real-time qPCR

Total RNA was extracted using TRIzol® Reagent (Invitrogen, Carlsbad, CA, USA). cDNA synthesis was conducted using SuperScript™ VILO™ cDNA Synthesis Kit (11754050, Invitrogen) with 2 μg of total RNA following the manufacturer's instructions. Quantitative real-time PCR was performed with SYBR Premix Ex Taq II (Takara, Japan) on an Mx3000P real-time PCR system (Stratagene). Ct values were analyzed using the comparative Ct ($^{\Delta\Delta Ct}$) method. The primer sequences used are listed in Table S4.

Immunofluorescence (IF) staining

Immunofluorescence staining of zebrafish embryos was carried out with established protocols[22]. Firstly, the zebrafish embryos in methanol rehydrate to PBST gradually. The embryos were incubated with 1 mM EDTA (pH 8.0) for antigen repair in a microwave when embryos became transparent, followed by blocking with inactivated goat serum. Primary antibody was added and incubated with embryos at 4 °C overnight, followed by PBST washing three times for 15 min each. After that, embryos were incubated with secondary antibody at 1:200 for 1 h at room temperature and then washed three times for 15 min each in PBST. DAPI was added (1 μg/ml) and incubated with embryos for 5 min at room temperature. Following washing three times with PBST, the embryos were mounted in 2% methylcellulose and observed under a confocal microscope (Nikon A1R+). The primary antibodies used were was listed in Table S3.

TUNEL staining

Zebrafish embryo samples were fixed and stained with a TUNEL staining kit (12156792910, Roche), according to the manufacturer's instructions. After fixation, the embryos were washed with PBST buffer again, and then permeabilized with 0.1% Triton X-100 to increase the permeability of the cell membrane so that the TdT enzyme could enter the cell. After pretreatment, the embryos were incubated with the TUNEL reaction mixture. TdT enzyme and rhodamine-labeled dUTP were added to the sample and prepared in the proportion recommended by the kit. The incubation condition was 37 ° C for 1 h. After incubation, the samples were washed three times with PBST for 5 min each time to remove the unbound dUTP and TdT enzymes.

BrdU staining

For BrdU incorporation assays, WT and *gdf11* mutant embryos at 46 hpf were incubated in 10 mM BrdU (B5002, Sigma-Aldrich) for 30 min at 4 °C. The embryos were then transferred to Holtfreter's solution to develop to 48 hpf, and BrdU incorporation was detected using an anti-BrdU antibody (1:1000; B5002, Sigma) following immunofluorescence experiments.

RNA deep sequencing

WT and *gdf11*$^{-/-}$ embryos in a *Tg(chd17-dsRed)* background were collected at 24 hpf, and these embryos were sorted using flow cytometry. These cells were subsequently sequenced by SHBIO Technology Company (Shanghai, China). Total RNA was extracted using TRIzol® Reagent (Invitrogen, Carlsbad, CA, USA). NEBNext rRNA depletion kit (New England Biolabs) was used to purify mRNA. NEBNext Ultra RNA Library Prep Kit for Illumina (New England Biolabs) was employed to construct sequencing libraries. Illumina HiSeq 2500 was used to read these libraries, and reads were mapped to the zebrafish GRCz10 genome using TopHat v2.0.12. We calculated FPKM values to determine gene expression levels.

SRI-011381 treatment

SRI-011381 (HY-100347 A, MCE) was dissolved in DMEM at a concentration of 10 μM for 6 h prior to cell lysis for Western blotting or IF. For rescue experiments, SRI-011381 was dissolved in Holtfreter's solution, and WT or *gdf11* mutant embryos were treated with 20 μM SRI-011381 from the one-cell stage to the indicated developmental stage[23].

Statistical analysis

Comparisons among multiple groups were analyzed using Student's t-tests in GraphPad Prism 9.4 (GraphPad Software, Inc., San Diego, CA, U.S.A.). Unpaired two-tailed t-tests were used for comparisons between different groups. Values are reported as mean ± SD. "*" $p < 0.05$ was considered to indicate a statistically-significant difference, very significant at $p < 0.01$ and labeled with "**", and extremely significant at $p < 0.001$ and labeled with "***".

Results

The functions of pronephros and cloaca were impaired after *gdf11* deletion

Previous studies report that Gdf11 deletion results in kidney absence in mice[24], with Gdf11 expression also observed in the hindgut[15]. However, the downstream mechanism by which Gdf11 regulates pronephros and cloaca development remains largely unknown. In prior research, we generated *gdf11* mutants in zebrafish and observed that the pronephric duct appeared narrower in *gdf11* mutants compared to WT embryos[18]. Additionally, a significant percentage of *gdf11* mutants exhibited malformations at the phrephros -cloaca area, as observed in bright-field microscopy (Fig. 1A). To further analyze pronephric duct and cloaca morphology, we used anti-atypical PKC (aPKC) to highlight the apical surface of pronephros and cloaca according to previous report[25]. Consistent with previous observations, *gdf11* mutants displayed pronephric stenosis accompanied by cloaca malformations (Fig. 1B). Given the morphological defects in the pronephros and cloaca of *gdf11* mutants, we investigated whether these structures retained normal function following *gdf11* deletion. At approximately 48 hpf, the pronephros attains functionality and commences the process of filtering the circulation[26]. We conducted a fluid excretion assay to evaluate renal function in *gdf11* knockout embryos, in accordance with previously established protocols[27]. Our results showed that *gdf11* mutants cleared fluids more slowly than WT embryos (Fig. 1C and D). To further assess cloaca function, we injected fluorescent rhodamine dextran into the anterior gut of embryos, following established methods[11]. While both WT and *gdf11*$^{-/-}$ embryos exhibited peristalsis, the mutant embryos were unable to excrete dextran through the cloaca (Fig. 1E and Supplementary Movies 1, 2). These findings indicate that Gdf11 is essential for maintaining the normal function of the pronephros and cloaca.

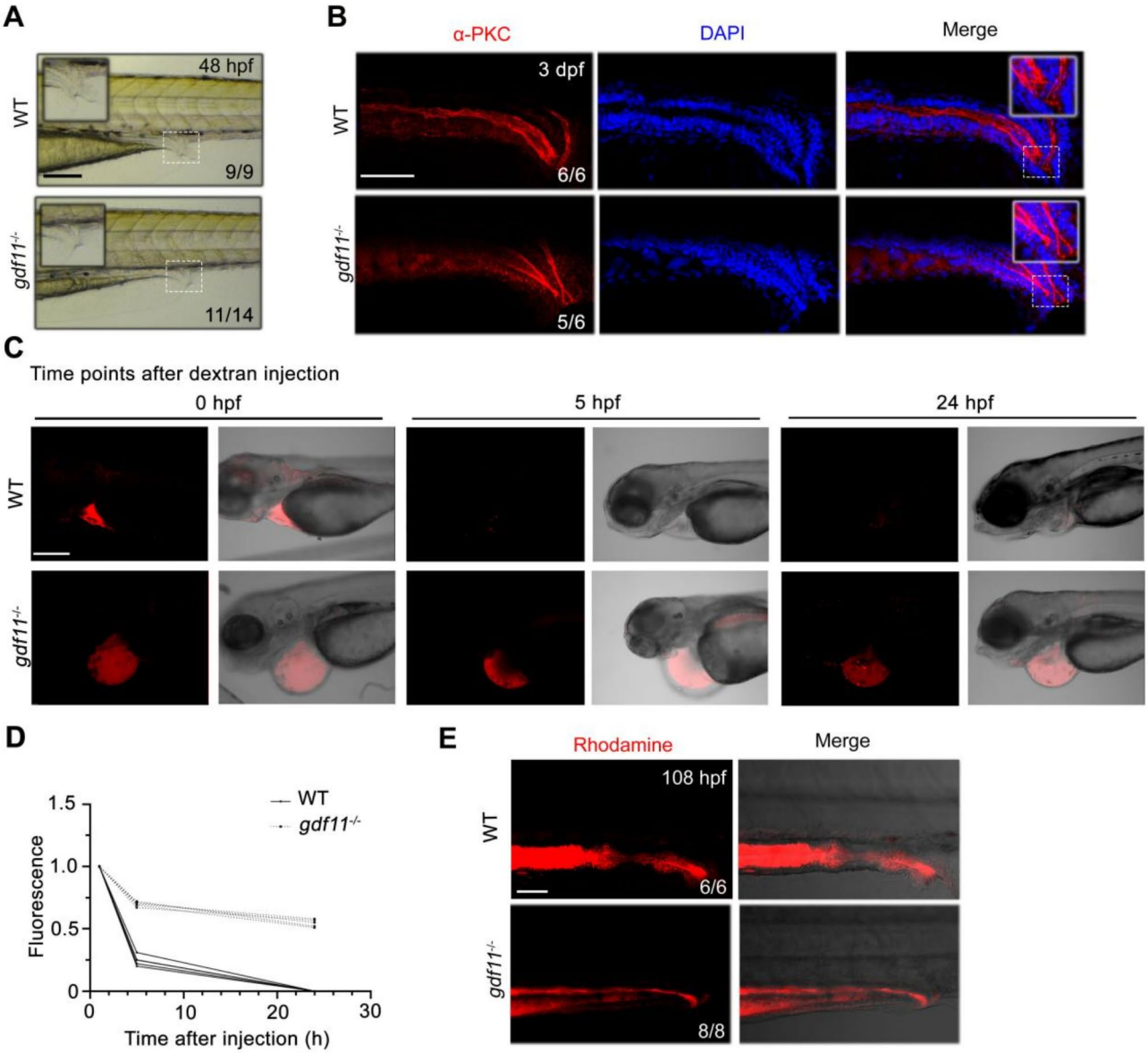

Fig. 1. *gdf11* knockout disrupts the function of the pronephros and cloaca in zebrafish. (**A**) Lateral view of pronephric tubules and cloaca at 36 hpf in WT and *gdf11*$^{-/-}$ mutants. Scale bar: 200 µm. (**B**) Lateral view of immunofluorescence images of α-PKC staining in both wild-type and *gdf11* mutant embryos. Scale bar: 100 µm. (**C**,**D**) *gdf11* mutant embryos exhibit slower clearance of dextran compared to WT embryos. Confocal images of embryos injected with 40 kDa rhodamine-dextran in the pericardial area immediately, and at 5–24 h post-injection (**C**). Quantification of fluorescence intensity (**D**). Scale bar: 50 µm. (**E**) Wild-type embryos rapidly secrete rhodamine dextran from the cloaca within minutes, while *gdf11* mutants excrete only minimal dye. Scale bar: 50 µm.

gdf11 knockout comprises the development of pronephros and cloaca

Given the morphological and functional defects observed in the pronephros and cloaca of *gdf11* mutants, we examined the developmental progression of these structures following *gdf11* knockout. Hematoxylin-Eosin staining revealed that *gdf11* deletion led to reduced glomeruli size and dilation of the pronephric tubules and ducts (Fig. 2A). The transcription factor *cdh17*, known to mark early epithelial development in the pronephric tubule and ducts[28], was assessed using a transgenic fish line expressing dsRed in the pronephric tubule and duct (*cdh17-dsRed*). This analysis showed a significant reduction of *cdh17* expression in *gdf11* mutants at 48 hpf (Fig. 2B). The zebrafish pronephros comprises paired glomeruli and two pronephric tubules/ducts, which eventually fuse with the cloaca[29]. WISH experiments utilizing *nephrin* and *wt1a* probes, which mark early pronephric glomerulus development at 48 hpf[30,31], revealed a significant decrease in *nephrin* and *wt1a* expression within the developing glomerulus following *gdf11* knockout (Fig. 2C). Nephrons, the functional units of the kidney, consist of segments that regulate fluid balance, osmolarity, and metabolic waste disposal[32]. We employed

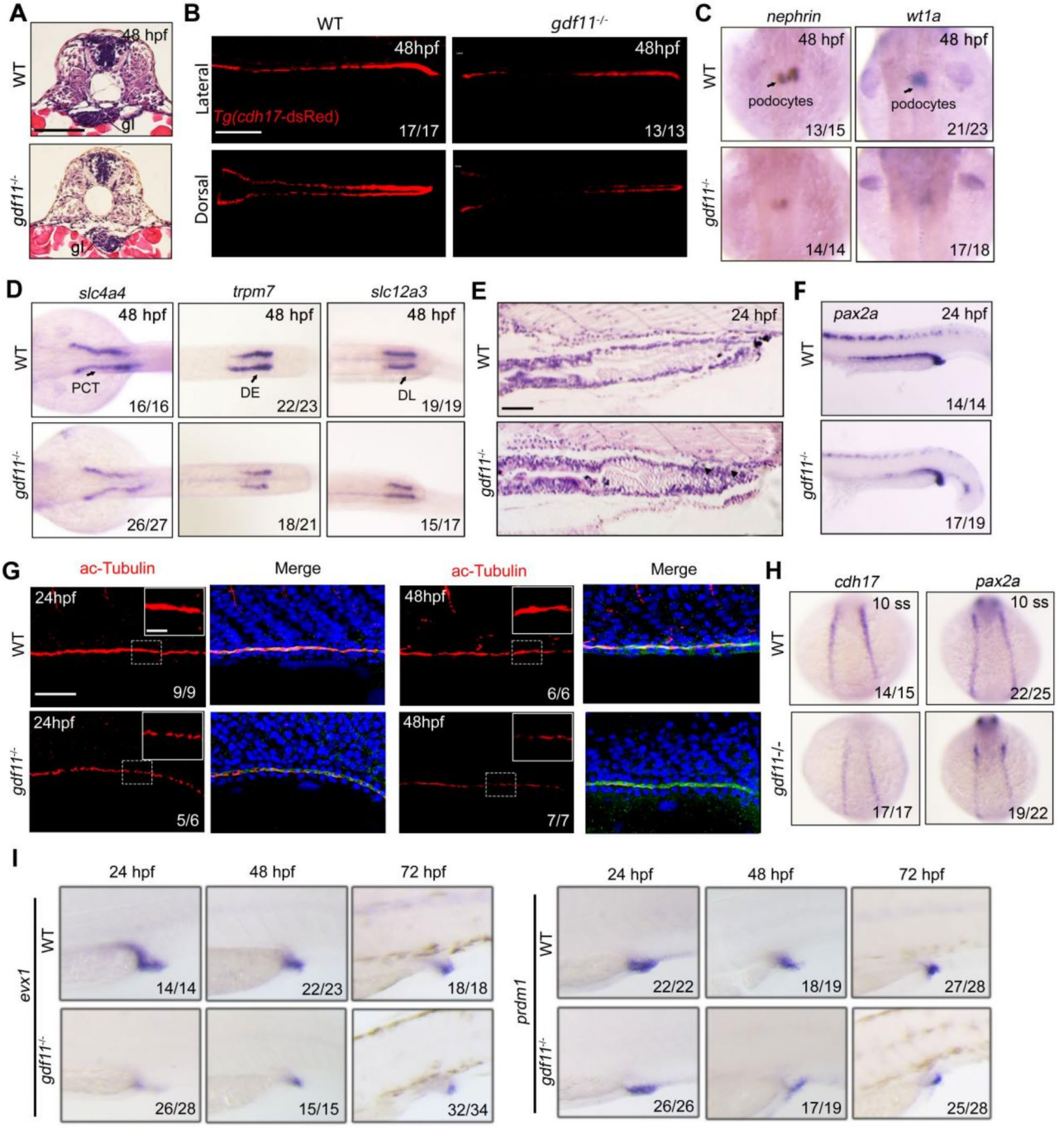

Fig. 2. *gdf11* is essential for pronephric tubule and cloaca organogenesis. (**A**) Hematoxylin-Eosin stained sections of WT and *gdf11* mutant larvae at the level of the glomerulus and proximal tubules at 48 hpf. Scale bar: 50 µm. (**B**) The expression of *cdh17* in WT and *gdf11* mutants under *Tg (cdh17-dsRed)* background. Scale bar: 200 µm. (**C**) In situ hybridization of *nephrin* (left) and *wt1a* (right) in wild-type and *gdf11* mutant embryos at 48 hpf. (**D**) WISH analysis in WT and *gdf11* mutants at 48 hpf for *slc4a4*, *trpm7*, and *slc12a3* probes. (**E**) H&E staining of the pronephric duct and cloaca region in WT and *gdf11* mutants at 48 hpf. Scale bar: 200 µm. (**F**) In situ hybridization with *pax2a* in WT and *gdf11* mutants at 24 hpf. (**G**) Confocal images showing cilia specification in WT and mutant embryos at 24 hpf and 48 hpf. Scale bar: 50 µm. (**H**) Comparative in situ hybridization of *cdh17* and *pax2a* expression in WT and *gdf11* mutants at 10 ss. (**I**) WISH analysis for *evx1* and *prdm1* in WT and *gdf11* mutants from 24 hpf to 72 hpf.

slc4a4, *trpm7*, and *slc12a3* to respectively label PCT, DE, and DL[9]. Our findings revealed that the expression of these marker genes was notably diminished and exhibited discontinuity in *gdf11* mutants (Fig. 2D and Fig. S1A). Additionally, Hematoxylin-Eosin staining confirmed the presence of pronephric stenosis in *gdf11* mutants (Fig. 2E). *pax2a*, which is expressed in the lateral cells of the pronephric primordium[33], showed significantly

reduced expression in *gdf11* mutants at 24 hpf (Fig. 2F). Based on these findings, we further examined pronephros cell differentiation following *gdf11* knockout. In the pronephric tubules, primary cilia are located on the epithelial cells of tubules[34,35]. Immunofluorescence analysis using α-PKC and acetylated-Tubulin in *gdf11* mutants with pronephric stenosis revealed pronephric duct dilations and disrupted cilia distribution, suggesting that cell differentiation within the pronephric tubules was significantly impaired in *gdf11*$^{-/-}$ mutants (Fig. 2G). The intermediate mesoderm, situated between the somite and lateral plate mesoderm, gives rise to pronephros progenitors[36]. Given the preceding data, we assessed *cdh17* and *pax2a* expression at the somite stage, finding that *gdf11* knockout led to defects in the intermediate mesoderm or presumptive pronephric mesoderm (Fig. 2H and Fig. S1B). Finally, we investigated tissue specification in the cloaca region by evaluating the expression of two cloacal markers from 24 hpf to 72 hpf, including *prdm1* and *evx1*[37,38]. Expression of these cloacal marker genes was reduced in mutant embryos compared to WT embryos (Fig. 2I and Fig. S1C). In summary, these findings indicate that *gdf11* deletion results in aberrant development of the pronephros and cloaca.

Suppression of *gdf11* expression also leads to pronephros and cloaca developmental defects

To verify the role of *gdf11* in pronephros and cloaca formation during embryonic development, we used a previously validated translation-blocking MO targeting the start codon of zebrafish *gdf11*, known to be essential for liver development in zebrafish[39]. To assess the knockdown efficiency, we constructed a plasmid containing part of the 5'-UTR and the open reading frame of *gdf11*, tagged with GFP. Co-injection of this plasmid with a control MO produced green fluorescence in zebrafish embryos. However, when co-injected with the *gdf11* translation-blocking MO, fluorescence was effectively suppressed, indicating successful knockdown of *gdf11* expression by the MO (Fig. 3A). To further confirm *gdf11* knockdown, we examined Gdf11 protein levels in embryo lysates injected with control or *gdf11* MO. Western blot analysis revealed a significant reduction in Gdf11 protein levels upon *gdf11* MO injection (Fig. 3B). Injection of *gdf11* MO at the one-cell stage produced notable embryonic defects, including pronephric stenosis, pericardial edema, hydrocephalus, reduced eye size, shorter body length, and cloaca malformation from 36 hpf to 72 hpf, consistent with previous reports (Fig. 3C)[40]. Importantly, these phenotypes induced by *gdf11* knockdown could be rescued with 200 pg of full-length *gdf11* mRNA, demonstrating the specificity of the *gdf11* MO (Fig. 3C). The development of the glomerulus and pronephric tubule was also disrupted in *gdf11* morphants, consistent with our earlier findings (Fig. 3D,E, Fig. S2A,B). WISH and real-time qPCR analyses indicated that *gdf11* also affected cloaca formation (Fig. 3F and Fig. S2C). These results confirm that the developmental defects in the pronephric tubule and cloaca arise specifically due to suppression or deletion of *gdf11* expression.

The cell death of pronephros and cloaca was severely affected when *gdf11* was deleted

During development, pronephric duct cells migrate toward the proctodeum epidermal cells, after which the pronephric duct tip cells continue migrating until they reach the cloaca. Some epidermal cells undergo apoptosis to help shape the pronephric duct or cloacal opening during this process[41]. To investigate apoptosis in pronephric duct and cloaca cells, we performed a TUNEL assay. In wild-type embryos, apoptosis occurred normally in both the pronephric ducts and cloaca; however, in *gdf11* mutant embryos, apoptosis was significantly reduced (Fig. 4A,B). We also analyzed cell proliferation in the pronephric ducts and cloaca of both wild-type and *gdf11* mutant embryos, finding no differences in proliferation between wild-type and mutant embryos (Fig. 4C,D). The BrdU incorporation experiments showed no change in pronephric and cloaca cells that excluded the problem with cell proliferation, and these data suggest that the malformation of pronephric ducts and cloaca was mainly due to defective apoptosis.

TGF-β signal acts downstream of *gdf11* regulating pronephric tubule and cloaca development

In zebrafish, pathways involving Notch, retinoic acid, Yap, and Wnt signaling contribute to pronephric kidney formation[25,42–44], while Wnt and Hedgehog signaling are reported to regulate cloaca formation[11–13,45]. To identify signaling pathways or genes with altered expression in pronephros and cloaca in the absence of Gdf11, we analyzed transcriptomic changes using RNA deep sequencing on WT and *gdf11* mutant embryos in *Tg(cdh17-dsRed)* background at 24 hpf. The heatmap displayed overall gene expression changes in the pronephros and cloaca tissue of *gdf11*$^{-/-}$ mutants compared to control embryos (Fig. S3). A volcano plot further highlighted genes that were significantly up- or down-regulated in *gdf11*$^{-/-}$ pronephric tubule/cloaca tissues relative to wild type (Fig. 5A). Gene ontology (GO) enrichment analysis of down-regulated genes revealed the TGF-β, AKT, MAPK, and Wnt pathways were among the most affected signals in *gdf11* mutants (Fig. 5B). Given that *gdf11* is a member of the TGF-β superfamily and signals through type I and II receptor serine/threonine kinases[46,47], we hypothesized that *gdf11* primarily influenced pronephros and cloaca development through TGF-β signaling. To test this, we examined SMAD2/3 and ALK5 phosphorylation levels in WT and *gdf11*$^{-/-}$ pronephric duct lysates. Consistent with prior studies[48,49], we found that phosphorylation of SMAD2/3 and ALK5 was significantly reduced in *gdf11*$^{-/-}$ pronephric duct lysates, while SMAD7, an inhibitory SMAD, was significantly elevated in mutant lysates (Fig. 5C). SRI-011381, an agonist of the TGF-β/Smad signaling pathway, is known to promote Smad2 and Smad3 phosphorylation and reduce SMAD7 expression[50]. We transfected Flag-zGdf11 into HEK 293T cells, with and without SRI-011381 treatment. Overexpression of zGdf11 notably increased the levels of p-Smad2 and p-Smad3, and this effect was further amplified by SRI-011381. SMAD7 levels were significantly reduced following Gdf11 overexpression, with an additional decrease upon SRI-011381 treatment (Fig. 5D). Given these findings, we conducted subcellular localization experiments in HEK 293T cells. In cells treated with DMSO, Smad2 was primarily located in the cytoplasm. However, upon Flag-Gdf11 transfection, Smad2 translocated to the nucleus. Additionally, Smad2 protein levels increased, and its nuclear localization significantly raised with SRI-011381 treatment (Fig. 5E). To further explore these effects, we treated WT and mutant embryos

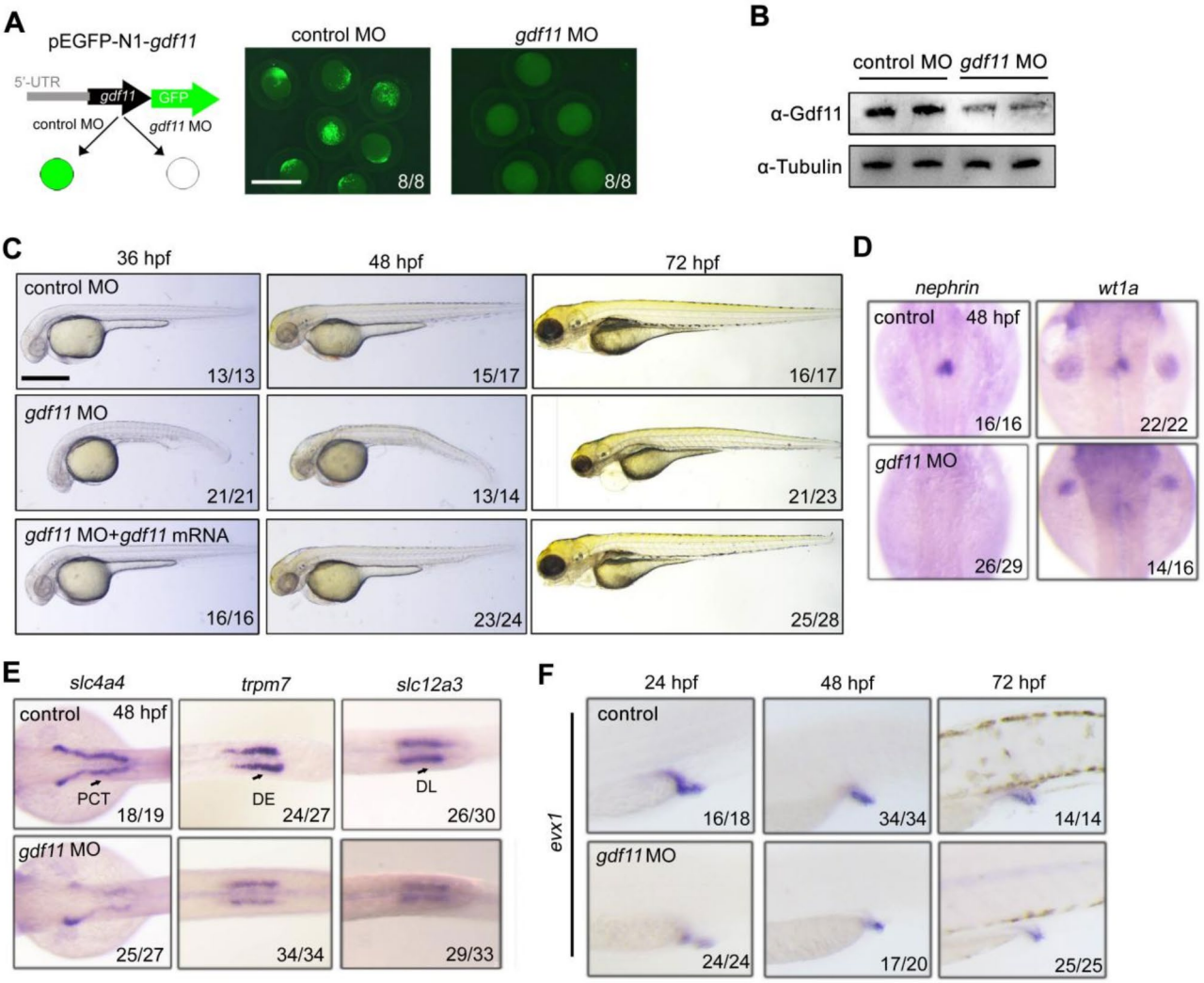

Fig. 3. *gdf11* knockdown disrupts pronephros and cloaca organogenesis. (**A**) Schematic representation of the plasmid used to test *gdf11* MO efficiency. Scale bar: 500 µm. (**B**) Western blot showing a significant reduction of Gdf11 protein levels in *gdf11* morphants. (**C**) Live imaging of control and *gdf11* morphants, with or without *gdf11* mRNA injection, from 36 hpf to 72 hpf. Scale bar: 300 µm. (**D**) Control and *gdf11* morphant embryos harvested at 48 hpf were subjected to WISH for *nephrin* and *wt1a* expression. (**E**) ISH analysis using segment-specific probes for the pronephric tubules in control and *gdf11* morphants at 48 hpf. (**F**) Lateral views of *evx1* expression in control and *gdf11* morphants from 24 hpf to 72 hpf.

with and without SRI-011381. After treatment, these embryos were harvested for WISH experiments targeting pronephros and cloaca-related probes. Our results showed that SRI-011381 treatment effectively restored pronephric tubules, /cloaca development and function (Fig. 5F-H and Fig. S4-5). Collectively, these findings strongly indicate that Gdf11 is crucial for pronephros and cloaca development, potentially through TGF-β signaling.

Discussion

Our study demonstrates that Gdf11 deletion or suppression disrupts pronephros and cloaca formation via the TGF-β signaling pathway in zebrafish, with these developmental defects being partially reversed through treatment with a TGF-β agonist (Fig. 6). Essential roles of *gdf11* in embryonic patterning, development, and kidney organogenesis have been previously validated through targeted Gdf11 deletion or knockdown[15,18,51]. Gdf11 plays an essential role in directing the initial outgrowth of the ureteric bud from the Wolffian duct, but the formation of the pronephros/mesonephros proceeds normally in mice lacking Gdf11 [24]. Based on that, we wonder whether the function of Gdf11 in zebrafish pronephros is unique in anamniotes. Recently, it has been reported that inhibition of SMAD2/3 signaling by SB431542 increased Wt1 expression, and inhibition of TGF-ß signaling may be required for induction of Wullerian duct mesenchymal cells from mesonephros[52]. Activin, a Gdf11 related ligand, in combination with retinoic acid, induces the formation of the pronephros[53]. However, Activin A is an endogenous inhibitor of ureteric bud outgrowth from the Wolffian duct[54]. We speculated Gdf11

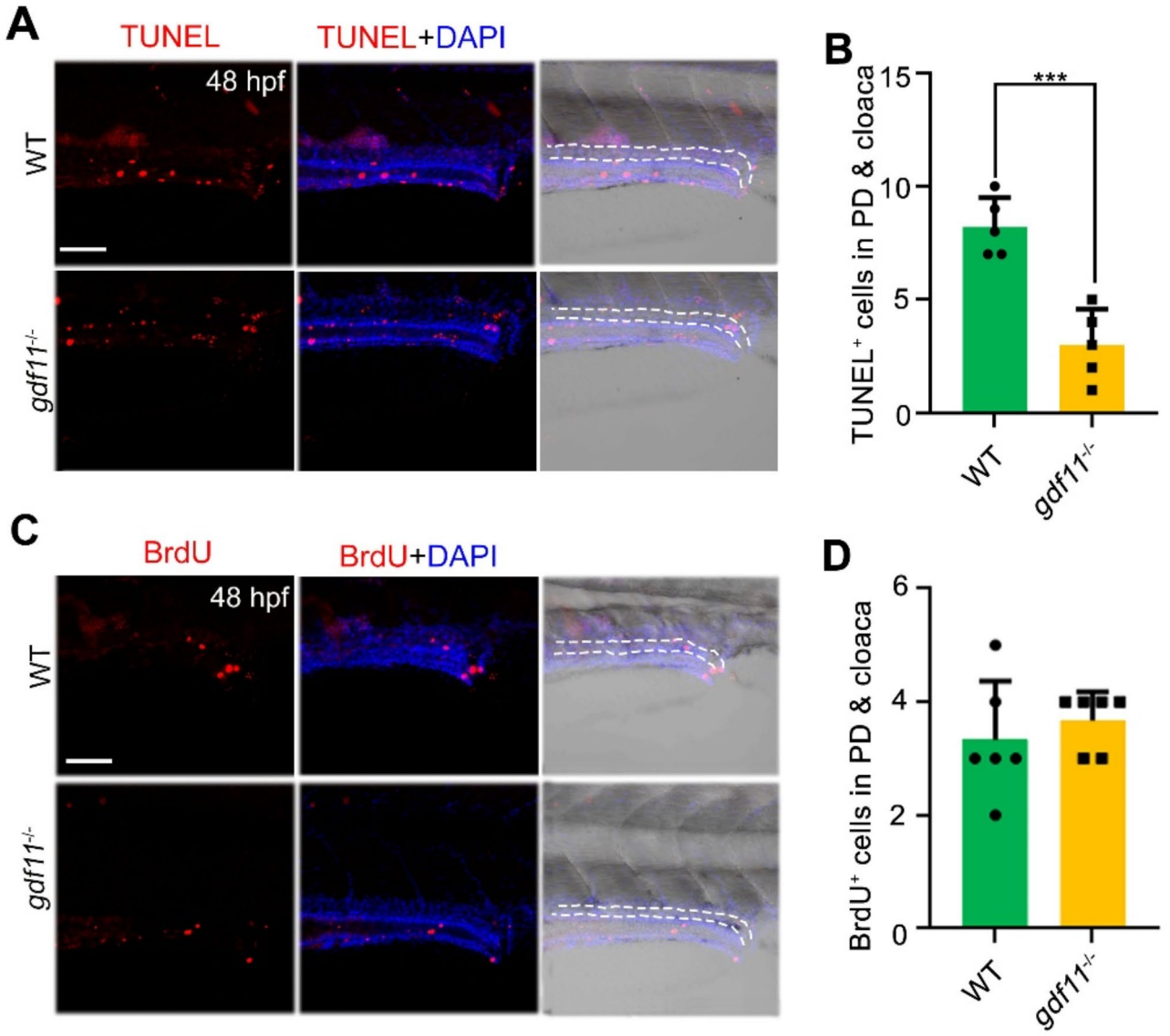

Fig. 4. The apoptosis of pronephric tubules and cloaca was significantly decreased upon *gdf11* deletion. (**A**,**B**) TUNEL assay showing decreased apoptosis in cells of the developing pronephric duct and cloaca in *gdf11* mutants. The position marked by the dotted line in the figure is the pronephros and the cloaca. Scale bar: 50 μm. (**C**,**D**) Cell proliferation, indicated by BrdU staining, remains unchanged in both WT and *gdf11* mutants. The position marked by the dotted line in the figure is the pronephros and the cloaca. Scale bar: 50 μm.

and Activin activity could induce pronephros formation, but Gdf11/Activin activities and SMAD2/3 signaling were inhibited at pronephros development stage. Further, Gdf11 inhibited metanephros formation and Activin inhibited mesonephros induction. In anamniotes, Gdf11 and SMAD2/3 signaling were not inhibited to facilitate pronephros formation. However, this hypothesis needs further validation.

However, the specific mechanisms of *gdf11* in kidney development remain only partially understood. GDF11 exerts developmental effects at least partly through binding to TGF-β/activin type I (TGFBR1/ALK5) and type II (ACVR2A, ACVR2B) receptors[47]. Due to the lethality associated with Gdf11 null mice, we utilized zebrafish as a model to investigate the downstream molecular mechanisms through which Gdf11 regulated pronephros organogenesis[47]. Our findings provide direct evidence that Gdf11 influences pronephros development via TGF-β and its downstream signaling.

It has been reported that the expression of GDF11 in the hindgut region of mouse embryos was crucial for hindgut organogenesis[17]. However, we did not detect significant *gdf11* expression in the pronephros or cloaca of zebrafish, suggesting that *gdf11* may function in these regions through indirect mechanisms.

In zebrafish, *gdf11* MO was previously used to study the regulation of liver growth and the posterior displacement of the pelvic fin[39,40]. Additionally, the *gdf11* loss-of-function mutant has been generated, displaying

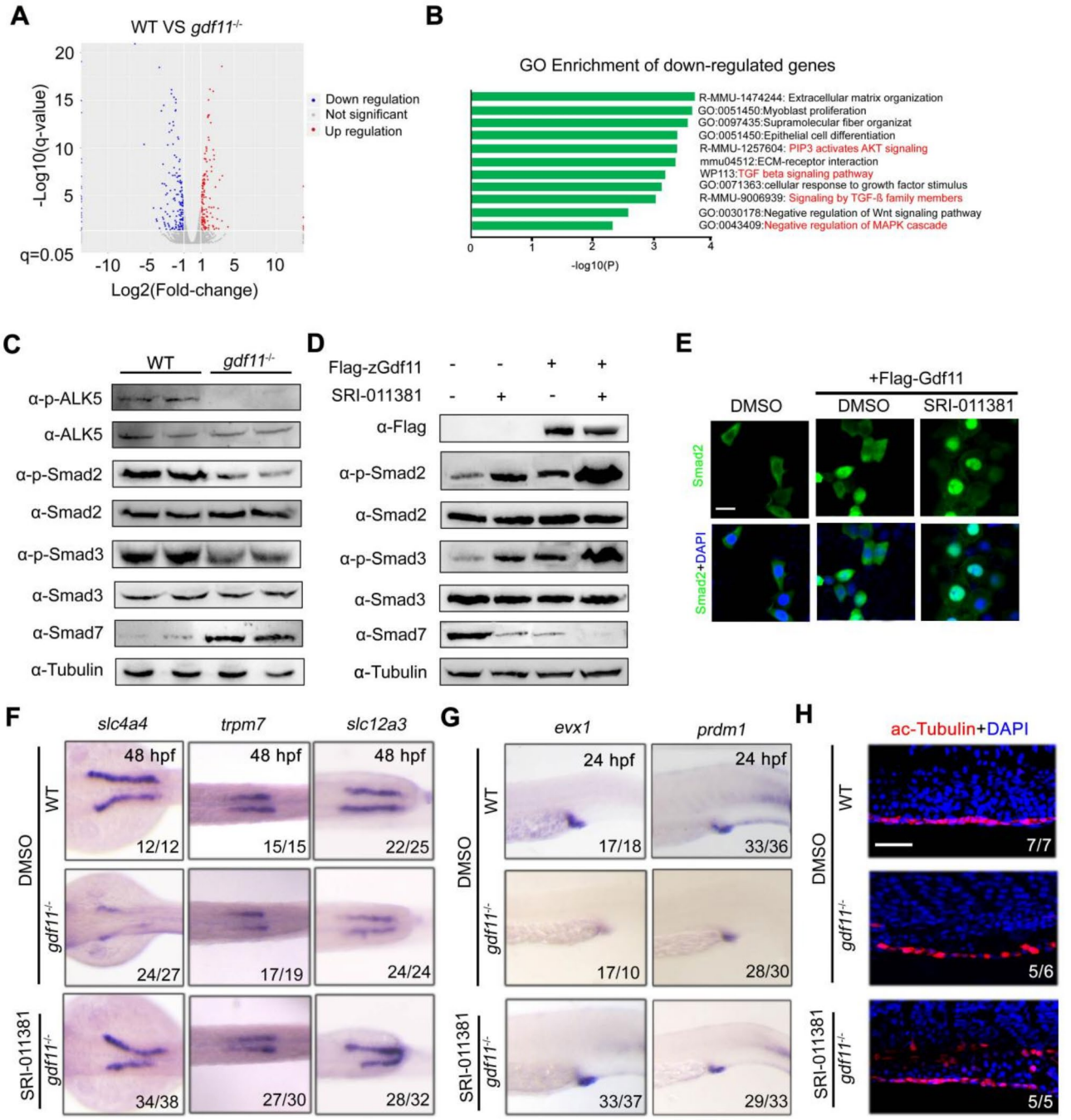

Fig. 5. TGF-β signaling acts downstream of Gdf11 promoting pronephros and cloaca formation. (**A**) Volcano plot highlighting differentially expressed genes in WT and *gdf11*$^{-/-}$ pronephros. (**B**) Gene Ontology analysis of biological processes using down-regulated differentially expressed genes. (**C**) Western blot showing key proteins of the TGF-β/Smad signaling pathway in WT and *gdf11*$^{-/-}$ mutant pronephros/cloaca lysates. (**D**) Comparative expression of key TGF-β/Smad pathway proteins following Gdf11 overexpression or SRI-011381 treatment in HEK 293T cells. (**E**) Subcellular localization of Smad2 in Flag-Gdf11-infected cells with or without SRI-011381 treatment. Scale bar: 50 μm. (**F**) Partial rescue of pronephros developmental defects in *gdf11* mutants by SRI-011381 treatment. (**G**) Partial rescue of cloaca developmental defects in *gdf11* mutants by SRI-011381 treatment. (**H**) Partial rescue of cilia in pronephric duct in *gdf11* mutants by SRI-011381 treatment. Scale bar: 50 μm.

disrupted craniofacial element arrangement, posteriorized pelvic fin, and disrupted left-right asymmetry[18,55]. However, pronephros and cloaca morphology were not characterized in these earlier reports.

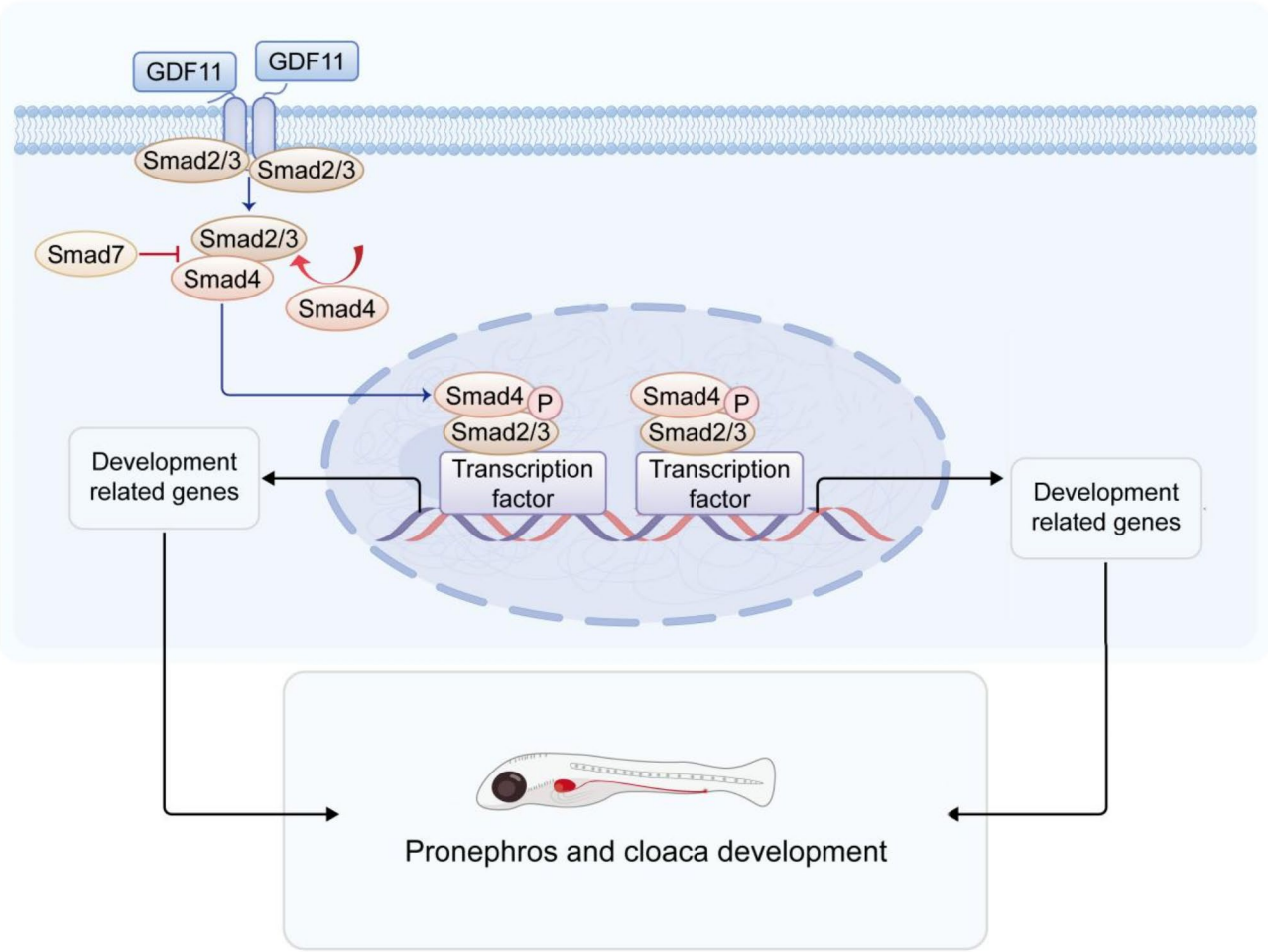

Fig. 6. Schematic of TGF-β signaling downstream of Gdf11 in pronephros and cloaca organogenesis. Gdf11 enhances TGF-β signaling, supporting pronephros and cloaca development. This schematic highlights Gdf11's essential role in zebrafish, illustrating the molecular mechanisms regulated by Gdf11.

Our study also observed reduced Wnt signaling activity in the pronephros of *gdf11* mutants. Prior studies have documented interactions between the TGF-β and Wnt pathways, for instance, GDF11 treatment has been shown to inhibit adipogenesis and differentiation by activating both ALK5-Smad2/3 and Wnt/β-catenin pathways[48].

Despite these findings, our study has some limitations. First, we examined the entire pronephros to study the impact of *gdf11* on its formation. Given that different renal cell types may respond variably to *gdf11* deletion, single-cell sequencing of isolated renal cell types should be employed in future studies to reveal the specific effects of *gdf11* deletion. Lastly, while we identified TGF-β signaling as the downstream pathway of *gdf11* in pronephros and cloaca formation, the direct target genes involved in these processes remain to be clarified in future investigations.

In this study, we have developed and characterized a novel zebrafish model with *gdf11* deficiency, exhibiting pronephros and cloaca malformations. Our findings demonstrate that *gdf11* is crucial for the development of renal and cloacal progenitors, acting upstream of the TGF-β signaling pathway. This model provides valuable insights into the genetic basis of related renal diseases and offers an innovative tool to further explore the roles of TGF-β signaling in development.

Data availability

The original contributions of this study are described in detail in the article. Any additional inquiries can be directed to the corresponding authors. The RNA deep sequencing datasets generated and/or analyzed during the current study are available in the BioProject repository (https://www.ncbi.nlm.nih.gov/bioproject/PRJNA1186345), accession number: PRJNA1186345.

Received: 30 October 2024; Accepted: 28 February 2025
Published online: 07 March 2025

References

1. Dressler, G. R. The cellular basis of kidney development. *Annu. Rev. Cell. Dev. Biol.* **22**, 509–529. https://doi.org/10.1146/annurev.cellbio.22.010305.104340 (2006).
2. Wang, Y. P., Zhou, C. J. J. & Liu, Y. H. Wnt signaling in kidney development and disease. *Prog Mol. Biol. Transl.* **153**, 181–207. https://doi.org/10.1016/bs.pmbts.2017.11.019 (2018).
3. Mukherjee, M., Fogarty, E., Janga, M. & Surendran, K. Notch signaling in kidney development, maintenance, and disease. *Biomolecules* **9** https://doi.org/10.3390/biom9110692 (2019).
4. Kurtzeborn, K., Kwon, H. N. & Kuure, S. MAPK/ERK signaling in regulation of renal differentiation. *Int. J. Mol. Sci.* **20**, 1779. https://doi.org/10.3390/ijms20071779 (2019).
5. Pace, J., Paladugu, P., Das, B., He, J. C. & Mallipattu, S. K. Targeting STAT3 signaling in kidney disease. *Am. J. Physiol-Renal.* **316**, F1151–F1161. https://doi.org/10.1152/ajprenal.00034.2019 (2019).
6. Trueb, B., Amann, R. & Gerber, S. D. Role of FGFRL1 and other FGF signaling proteins in early kidney development. *Cell. Mol. Life Sci.* **70**, 2505–2518. https://doi.org/10.1007/s00018-012-1189-9 (2013).
7. Lan, H. Y. & Chung, A. C. K. TGF-β/Smad signaling in kidney disease. *Semin Nephrol.* **32**, 236–243. https://doi.org/10.1016/j.semnephrol.2012.04.002 (2012).
8. Wingert, R. A. et al. The Cdx genes and retinoic acid control the positioning and segmentation of the zebrafish pronephros. *PLoS Genet.* **3**, 1922–1938. https://doi.org/10.1371/journal.pgen.0030189 (2007).
9. Naylor, R. W., Qubisi, S. S. & Davidson, A. J. Zebrafish pronephros development. *Results Probl. Cell. Differ.* **60**, 27–53. https://doi.org/10.1007/978-3-319-51436-9_2 (2017).
10. Wang, H. et al. Inversin (NPHP2) and Vangl2 are required for normal zebrafish cloaca formation. *Biochem. Biophys. Res. Commun.* **673**, 9–15. https://doi.org/10.1016/j.bbrc.2023.06.058 (2023).
11. Pyati, U. J., Cooper, M. S., Davidson, A. J., Nechiporuk, A. & Kimelman, D. Sustained Bmp signaling is essential for cloaca development in zebrafish. *Development* **133**, 2275–2284. https://doi.org/10.1242/dev.02388 (2006).
12. Gredler, M. L., Patterson, S. E., Seifert, A. W. & Cohn, M. J. Foxa1 and Foxa2 orchestrate development of the urethral tube and division of the embryonic cloaca through an autoregulatory loop with Shh. *Dev. Biol.* **465**, 23–30. https://doi.org/10.1016/j.ydbio.2020.06.009 (2020).
13. Baranowska Korberg, I. et al. WNT3 involvement in human bladder exstrophy and cloaca development in zebrafish. *Hum. Mol. Genet.* **24**, 5069–5078. https://doi.org/10.1093/hmg/ddv225 (2015).
14. Zhang, Y. H. et al. Role of growth differentiation factor 11 in development, physiology and disease. *Oncotarget* **8**, 81604–81616. https://doi.org/10.18632/oncotarget.20258 (2017).
15. Esquela, A. F. & Lee, S. e.-J. Regulation of metanephric kidney development by growth/differentiation factor 11. *Dev. Biol.* **257**, 356–370. https://doi.org/10.1016/s0012-1606(03)00100-3 (2003).
16. Pons, M. et al. GDF11 induces kidney fibrosis, renal cell epithelial-to-mesenchymal transition, and kidney dysfunction and failure. *Surgery* **164**, 262–273. https://doi.org/10.1016/j.surg.2018.03.008 (2018).
17. Tsuda, T. et al. PCSK5 and GDF11 expression in the hindgut region of mouse embryos with anorectal malformations. *Eur. J. Pediatr. Surg.* **21**, 238–241. https://doi.org/10.1055/s-0031-1273691 (2011).
18. Yao, W., Wei, Z., Tian, X., Tan, J. & Liu, J. Gdf11 regulates left-right asymmetry development through TGF-beta signal. *Cell. Prolif.*. https://doi.org/10.1111/cpr.13765 (2024).
19. Farooq, M. et al. Histone deacetylase 3 is specifically required for liver development in zebrafish. *Dev. Biol.* **317**, 336–353. https://doi.org/10.1016/j.ydbio.2008.02.034 (2008).
20. Liu, J. W. et al. Chemokine signaling links cell-cycle progression and cilia formation for left-right symmetry breaking. *Plos Biol.* **17**, e3000203. https://doi.org/10.1371/journal.pbio.3000203 (2019).
21. Tobin, J. L. & Beales, P. L. Restoration of renal function in zebrafish models of ciliopathies. *Pediatr Nephrol* **23**, 2095–2099. https://doi.org/10.1007/s00467-008-0898-7 (2008).
22. Wei, Z., Hong, Q., Ding, Z. & Liu, J. cxcl12a plays an essential role in pharyngeal cartilage development. *Front. Cell. Dev. Biol.* **11**, 1243265. https://doi.org/10.3389/fcell.2023.1243265 (2023).
23. Liu, Y. et al. Saikosaponin A protects from pressure Overload-Induced cardiac fibrosis via inhibiting fibroblast activation or endothelial cell EndMT. *Int. J. Biol. Sci.* **14**, 1923–1934. https://doi.org/10.7150/ijbs.27022 (2018).
24. Esquela, A. F. & Lee, S. J. Regulation of metanephric kidney development by growth/differentiation factor 11. *Dev. Biol.* **257**, 356–370. https://doi.org/10.1016/s0012-1606(03)00100-3 (2003).
25. He, L. et al. Yes-associated protein (Yap) is necessary for ciliogenesis and morphogenesis during pronephros development in zebrafish (Danio Rerio). *Int. J. Biol. Sci.* **11**, 935–947. https://doi.org/10.7150/ijbs.11346 (2015).
26. Kramer-Zucker, A. G. et al. Cilia-driven fluid flow in the zebrafish Pronephros, brain and Kupffer's vesicle is required for normal organogenesis. *Development* **132**, 1907–1921. https://doi.org/10.1242/dev.01772 (2005).
27. Kotb, A. M. et al. Simultaneous assessment of glomerular filtration and barrier function in live zebrafish. *Am. J. Physiol. Ren. Physiol.* **307**, F1427–1434. https://doi.org/10.1152/ajprenal.00029.2014 (2014).
28. Zhou, W., Boucher, R. C., Bollig, F., Englert, C. & Hildebrandt, F. Characterization of mesonephric development and regeneration using Transgenic zebrafish. *Am. J. Physiol. Ren. Physiol.* **299**, F1040–1047. https://doi.org/10.1152/ajprenal.00394.2010 (2010).
29. Ebarasi, L., Oddsson, A., Hultenby, K., Betsholtz, C. & Tryggvason, K. Zebrafish: a model system for the study of vertebrate renal development, function, and pathophysiology. *Curr. Opin. Nephrol. Hypertens.* **20**, 416–424. https://doi.org/10.1097/MNH.0b013e3283477797 (2011).
30. Ichimura, K. et al. Developmental localization of nephrin in zebrafish and Medaka pronephric glomerulus. *J. Histochem. Cytochem.* **61**, 313–324. https://doi.org/10.1369/0022155413477115 (2013).
31. O'Brien, L. L. et al. Wt1a, Foxc1a, and the Notch mediator Rbpj physically interact and regulate the formation of podocytes in zebrafish. *Dev. Biol.* **358**, 318–330. https://doi.org/10.1016/j.ydbio.2011.08.005 (2011).
32. Wingert, R. A. & Davidson, A. J. The zebrafish Pronephros: a model to study nephron segmentation. *Kidney Int.* **73**, 1120–1127. https://doi.org/10.1038/ki.2008.37 (2008).
33. Majumdar, A., Lun, K., Brand, M. & Drummond, I. A. Zebrafish no isthmus reveals a role for pax2.1 in tubule differentiation and patterning events in the pronephric primordia. *Development* **127**, 2089–2098. https://doi.org/10.1242/dev.127.10.2089 (2000).
34. Zhang, Q., Liu, Q., Austin, C., Drummond, I. & Pierce, E. A. Knockdown of ttc26 disrupts ciliogenesis of the photoreceptor cells and the pronephros in zebrafish. *Mol. Biol. Cell.* **23**, 3069–3078. https://doi.org/10.1091/mbc.E12-01-0019 (2012).
35. Zhai, G. et al. Sept6 is required for ciliogenesis in Kupffer's vesicle, the Pronephros, and the neural tube during early embryonic development. *Mol. Cell. Biol.* **34**, 1310–1321. https://doi.org/10.1128/MCB.01409-13 (2014).
36. Davidson, A. J., Lewis, P., Przepiorski, A. & Sander, V. Turning mesoderm into kidney. *Semin Cell. Dev. Biol.* **91**, 86–93. https://doi.org/10.1016/j.semcdb.2018.08.016 (2019).
37. Wilm, T. P. & Solnica-Krezel, L. Essential roles of a zebrafish prdm1/blimp1 homolog in embryo patterning and organogenesis. *Development* **132**, 393–404. https://doi.org/10.1242/dev.01572 (2005).
38. Thaeron, C. et al. Zebrafish evx1 is dynamically expressed during embryogenesis in subsets of interneurones, posterior gut and urogenital system. *Mech. Dev.* **99**, 167–172. https://doi.org/10.1016/s0925-4773(00)00473-1 (2000).
39. Farooq, M. et al. Histone deacetylase 3 (hdac3) is specifically required for liver development in zebrafish. *Dev. Biol.* **317**, 336–353. https://doi.org/10.1016/j.ydbio.2008.02.034 (2008).

40. Murata, Y. et al. Allometric growth of the trunk leads to the rostral shift of the pelvic fin in teleost fishes. *Dev. Biol.* **347**, 236–245. https://doi.org/10.1016/j.ydbio.2010.07.034 (2010).
41. Nguyen, T. K., Petrikas, M., Chambers, B. E. & Wingert, R. A. Principles of zebrafish nephron segment development. *J. Dev. Biol.* **11** https://doi.org/10.3390/jdb11010014 (2023).
42. Liu, Y., Pathak, N., Kramer-Zucker, A. & Drummond, I. A. Notch signaling controls the differentiation of transporting epithelia and multiciliated cells in the zebrafish pronephros. *Development* **134**, 1111–1122. https://doi.org/10.1242/dev.02806 (2007).
43. Li, Y., Cheng, C. N., Verdun, V. A. & Wingert, R. A. Zebrafish nephrogenesis is regulated by interactions between retinoic acid, Mecom, and Notch signaling. *Dev. Biol.* **386**, 111–122. https://doi.org/10.1016/j.ydbio.2013.11.021 (2014).
44. Burckle, C. et al. Control of the Wnt pathways by nephrocystin-4 is required for morphogenesis of the zebrafish pronephros. *Hum. Mol. Genet.* **20**, 2611–2627. https://doi.org/10.1093/hmg/ddr164 (2011).
45. Parkin, C. A., Allen, C. E. & Ingham, P. W. Hedgehog signalling is required for cloacal development in the zebrafish embryo. *Int. J. Dev. Biol.* **53**, 45–57. https://doi.org/10.1387/ijdb.082669cp (2009).
46. Rochette, L., Zeller, M., Cottin, Y. & Vergely, C. Growth and differentiation factor 11 (GDF11): functions in the regulation of erythropoiesis and cardiac regeneration. *Pharmacol. Ther.* **156**, 26–33. https://doi.org/10.1016/j.pharmthera.2015.10.006 (2015).
47. Oh, S. P. et al. Activin type IIA and IIB receptors mediate Gdf11 signaling in axial vertebral patterning. *Genes Dev.* **16**, 2749–2754. https://doi.org/10.1101/gad.1021802 (2002).
48. Frohlich, J. et al. GDF11 inhibits adipogenesis and improves mature adipocytes metabolic function via WNT/beta-catenin and ALK5/SMAD2/3 pathways. *Cell. Prolif.* **55**, e13310. https://doi.org/10.1111/cpr.13310 (2022).
49. Honda, M. et al. Pathophysiological levels of GDF11 activate Smad2/Smad3 signaling and induce muscle atrophy in human iPSC-derived myocytes. *Am. J. Physiol. Cell. Physiol.* **323**, C1402–C1409. https://doi.org/10.1152/ajpcell.00341.2022 (2022).
50. Chen, C. et al. Ganoderma lucidum polysaccharide inhibits HSC activation and liver fibrosis via targeting inflammation, apoptosis, cell cycle, and ECM-receptor interaction mediated by TGF-beta/Smad signaling. *Phytomedicine* **110**, 154626. https://doi.org/10.1016/j.phymed.2022.154626 (2023).
51. Andersson, O., Reissmann, E. & Ibanez, C. F. Growth differentiation factor 11 signals through the transforming growth factor-beta receptor ALK5 to regionalize the anterior-posterior axis. *EMBO Rep.* **7**, 831–837. https://doi.org/10.1038/sj.embor.7400752 (2006).
52. Nakajima, T. et al. SMAD2/3 signaling regulates initiation of mouse wolffian ducts and proximal differentiation in mullerian ducts. *FEBS Open. Bio.* **14**, 37–50. https://doi.org/10.1002/2211-5463.13729 (2024).
53. Asashima, M., Ariizumi, T. & Malacinski, G. M. In vitro control of organogenesis and body patterning by activin during early amphibian development. *Comp. Biochem. Physiol. B Biochem. Mol. Biol.* **126**, 169–178. https://doi.org/10.1016/s0305-0491(00)00195-4 (2000).
54. Maeshima, A., Vaughn, D. A., Choi, Y. & Nigam, S. K. Activin A is an endogenous inhibitor of ureteric bud outgrowth from the wolffian duct. *Dev. Biol.* **295**, 473–485. https://doi.org/10.1016/j.ydbio.2006.03.011 (2006).
55. Ravenscroft, T. A. et al. Heterozygous loss-of-function variants significantly expand the phenotypes associated with loss of GDF11. *Genet. Med.* **23**, 1889–1900. https://doi.org/10.1038/s41436-021-01216-8 (2021).

Author contributions

JW. L. and ZL. H. designed the research; XN.T. performed all the experiments; WT. Y. and J. T. participated in the data analysis and contributed to writing; XN. T. , JW. L. and ZL. H. wrote the manuscript.

Funding

This work was supported by the National Natural Science Foundation of China (32300681), Anhui Province Scientific Research Plan Project (2023AH050657), Scientific research start-up funds of Anhui Medical University (0101045201), Anhui Medical University Clinical Medicine Discipline Construction Project (2020lcxk023) and Research Fund of Anhui Institute of Translational Medicine (2023zhyx-C77).

Declarations

Competing interests

The authors declare no competing interests.

Ethics declarations

All institutional and national guidelines for the care and use of animals (fisheries) were in accordance with the Guide for the Care and Use of Laboratory Animals and ARRIVE guidelines (https://arriveguidelines.org). The zebrafish experiments were approved by the Animal Ethics Committee of Anhui Medical University (permission number: LLSC-20231931).

Additional information

Supplementary Information The online version contains supplementary material available at https://doi.org/10.1038/s41598-025-92571-y.

Correspondence and requests for materials should be addressed to Z.H. or J.L.